SINDO1 Study of the Photoisomerization of 2-Methylfuran to 3-Methylfuran

Sabine Buss and Karl Jug*

Contribution from the Theoretische Chemie, Universität Hannover, 3000 Hannover, West Germany. Received August 25, 1986

Abstract: The mechanism of the photoisomerization of 2-methylfuran to 3-methylfuran was investigated with the semiempirical MO method SINDO1. The potential energy hypersurfaces of excited states were calculated with configuration interaction (CI). The actual photochemical reaction is preceded by a cascading sequence of internal conversion and intersystem crossing processes in the Franck–Condon zone. The reaction is then initiated by ring opening on the lowest triplet surface, followed by intersystem crossing to the singlet ground state. On the ground state surface, thermal reaction to the product occurs via an intermediate, 1-methylcyclopropene-3-carbaldehyde. The low experimental yield is explained by a reaction scheme, which contains various branchings leading back to the reactant.

I. Introduction

Characteristic for the photoisomerization of many five-membered heterocyclic aromatic systems is the occurrence of products formed by permutation of ring atoms. Most frequently the exchange of two neighboring atoms is observed. For different heterocycles these reactions differ in yields and byproducts. The permutations are assumed to proceed via different mechanisms dependent on the heteroatom in the ring. Essentially five mechanisms have been proposed as explanation for the different reactions.[1]

In furans atoms 2 and 3 are permuted.[1–12] The yield is low.
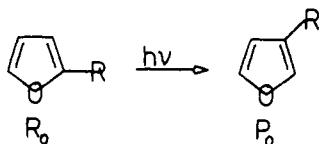
This permutation is explained by a reaction path, which includes a cyclopropenecarbaldehyde as an intermediate. This mechanism is called ring contraction–ring expansion.[1–12]
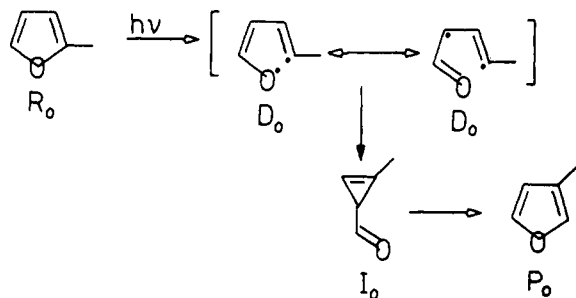
The first step in this reaction is the breaking of the O–C bond. In 2-alkylfurans there is a highly selective breaking of the O–C$_{(2)}$ bond. Previous theoretical papers on the photochemistry of other five-membered heterocycles have always treated unsubstituted systems.[13–15] In consequence the selectivity of the bond breaking due to substitution with an alkyl group remained unexplained. Nishimoto et al.[13] have reported about the ring contraction–ring expansion mechanism in an ab initio study of the photochemistry of isoxazole. They concluded from their calculations that ring expansion takes place in isoxazole on an excited potential energy hypersurface. On the other hand, Monti and Bertrand[16] found in experiments on methyl substituted furan derivatives that this reaction step occurs thermally, i.e., on the ground-state surface. Experiments show also that a triplet state is involved in this reaction.[1,2,12] Since direct excitation from the singlet ground state into the excited triplet state is spin forbidden, singlet–triplet crossings must occur during the reaction.

In this work we chose the photoisomerization of 2-methylfuran to 3-methylfuran as an example for the furan mechanism, because 2-methylfuran is the simplest 2-alkylfuran. There are two reasons for the selection of a substituted system. First it is interesting because of the high selectivity of bond breaking that demands an explanation and second because it offers the possibility of distinction between reactant and product. For the reactant and all isomers which occur during the reaction, potential energy hypersurfaces (PES) of excited states are calculated. The obtained information should serve for a better understanding of the mechanism of photochemical isomerization of 2-methylfuran (R_0) via 1-methylcyclopropene-3-carbaldehyde (I_0) as intermediate to 3-methylfuran (P_0) and the photochemical mechanism of furan derivatives in general.

II. Method of Calculation

The calculations were performed with the semiempirical MO method SINDO1.[17] This method has been successfully applied in the explanation of the reaction mechanism of photoisomerization and photofragmentation of other five- and three-membered ring systems, namely cyclopentanone[18] and substituted diazirines.[19]

The ground-state geometries of reactant 2-methylfuran, intermediate 1-methylcyclopropene-3-carbaldehyde, and product 3-methylfuran were localized on the SCF potential energy hypersurface by complete geometry optimization with a Newton-

(1) Padwa, A. *Rearrangements in ground and excited states*; De Mayo, P., Ed.; Academic: New York, 1980; Vol. 3.
(2) Hiraoka, H. *J. Phys. Chem.* **1970**, *74*, 574.
(3) Hiraoka, H.; Srinivasan, R. *J. Am. Chem. Soc.* **1968**, *89*, 2720.
(4) Srinivasan, R. *J. Am. Chem. Soc.* **1967**, *89*, 4812.
(5) Srinivasan, R. *J. Am. Chem. Soc.* **1967**, *89*, 1758.
(6) Couture, A.; Delevallee, A.; Lablache-Combier, A.; Pårkånyi, C. *Tetrahedron* **1975**, *31*, 785.
(7) Couture, A.; Lablache-Combier, A. *Chem. Commun.* **1971**, 891.
(8) Hiraoka, H. *Tetrahedron* **1973**, *29*, 2955.
(9) van Tamelen, E. E.; Whitesides, T. E. *J. Am. Chem. Soc.* **1968**, *90*, 3894.
(10) van Tamelen, E. E.; Whitesides, T. E. *J. Am. Chem. Soc.* **1971**, *93*, 6129.
(11) Boué, S.; Srinivasan, R. *J. Am. Chem. Soc.* **1970**, *92*, 1824.
(12) Srinivasan, R. *J. Pure Appl. Chem.* **1968**, *16*, 65.

(13) Tanaka, H.; Osamura, Y.; Matsushita, T.; Nishimoto, K. *Bull. Chem. Soc. Jpn.* **1981**, *54*, 1293.
(14) Tanaka, H.; Matsushita, T.; Nishimoto, K. *J. Am. Chem. Soc.* **1983**, *105*, 1753.
(15) Matsushita, T.; Tanaka, H.; Nishimoto, K.; Osamura, Y. *Theor. Chim. Acta* **1983**, *63*, 55.
(16) Monti, H.; Bertrand, M. *Tetrahedron Lett.* **1969**, *16*, 1235.
(17) Nanda, D. N.; Jug, K. *Theor. Chim. Acta* **1980**, *57*, 95.
(18) Müller-Remmers, P. L.; Mishra, P. C.; Jug, K. *J. Am. Chem. Soc.* **1984**, *106*, 2538.
(19) Müller-Remmers, P. L.; Jug, K. *J. Am. Chem. Soc.* **1985**, *107*, 7275.
(20) Jug, K.; Hahn, G. *J. Comput. Chem.* **1983**, *4*, 410.
(21) Himmelblau, D. A. *Applied Nonlinear Programming*; McGraw-Hill: New York, 1972.

Table I. Vertical Excitations of 2-Methylfuran (eV)

		energy	
		experimental	
state	calcd	in MeOH[27]	in gas phase[1]
$^3R_1(^3B_2)$	3.08		
$^3R_2(^3A_1)$	4.12		
$^3R_3(^3A_2)$	4.48		
$^3R_4(^3B_1)$	4.71		
$R_1(^1A_2)$	4.98 (w)	4.13 (w)	
$R_2(^1B_1)$	5.22 (w)	(4.90 (w))	
$R_3(^1B_2)$	6.32 (s)	5.84 (s)	6.03

Raphson procedure. Bond lengths were optimized to 0.001 Å and angles to 0.1°.

The vertical excitation energies were determined by configuration interaction (CI) with single excitations from the two highest occupied MOs into the four lowest virtual MOs. Excitations from lower lying occupied MOs or into higher lying virtual MOs had negligible coefficients in the CI eigenvectors for vertical excitation energies in the range of interest.

According to Salem[22] diradicals are characterized by a singlet–triplet degeneracy. If the lowest lying triplet state is located above the lowest singlet state, the energy of the triplet must be lowered or the energy of the singlet must be raised in a search for a diradical. Therefore we tried to locate the diradical in the neighborhood of the minimum of the lowest triplet. We used single and double excitations in the CI.

For the determination of the reaction path it was necessary to calculate the minima of the three lowest excited singlet states R_1, R_2, R_3 and the third triplet state $^3R_3$ in the Franck–Condon zone. For this purpose the CI which was used for the calculation of vertical energies was reduced. For each state only those Slater determinants were included whose coefficients were larger than 0.2 in the CI eigenvectors. We then added all those determinants which had CI coefficients larger than 0.2 in lower lying states of the same spin multiplicity. On these potential energy hypersurfaces complete geometry optimization was performed.

To guarantee the correct correlation of excited states at different geometries we proceeded as follows. The vertical excitations at the geometries of the minima of the excited states R_1, R_2, R_3, $^3R_3$, and $^3I_1$ were correlated with those of the reactant. The MOs resulting at such geometries were topologically compared with the MOs of the reactant R_0. Excitations were calculated from those MOs which correspond to the two highest occupied MOs of R_0, to those which correspond to the four lowest virtual orbitals of R_0. States calculated from this CI were correlated with the vertical excitations of reactant R_0.

In the reaction profile we use as abscissa a significant coordinate whose change reflects the reaction course. For the considered reaction there are two significant lengths: the $O–C_{(2)}$ distance which increases and the $O–C_{(3)}$ distance which decreases. By these two lengths we can describe the initial opening and the final closing of bonds. The use of only one of the coordinates as abscissa would result, particularly in the Franck–Condon zone in a rather badly arranged, hard to interpret reaction profile. Here the reaction path is presented in the coordinate diagram of both coordinates. In this diagram the two coordinates are used as the two axes. In this coordinate system we put all points which are passed through during the reaction. These points are the minima on the excited hypersurfaces mentioned above and calculated by complete geometry optimization. We connect these points linearly in the sequence in which they are passed through. In this fashion the reaction pathway is obtained. This reaction pathway is topologically mapped on a line which represents the abscissa for the reaction profile. The reaction profiles are evaluated and the result is presented in the reaction scheme.

III. Results and Discussion

1. Ground-State Geometries. The equilibrium geometries of reactant 2-methylfuran (R_0), intermediate 1-methylcyclo-
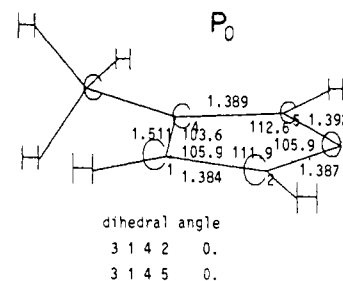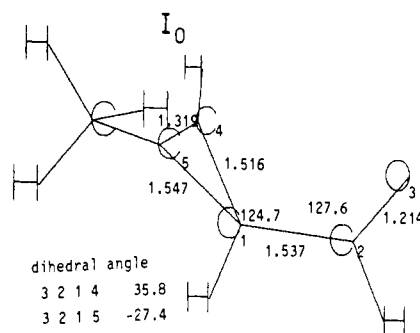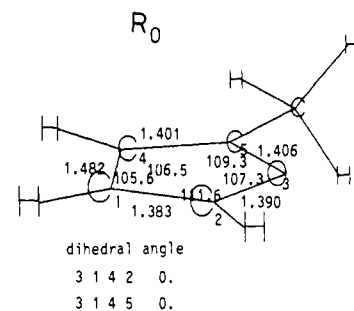

Figure 1. Geometry of ground states R_0, I_0, and P_0.

propene-3-carbaldehyde (I_0), and product 3-methylfuran (P_0) were localized on the SCF hypersurface. They are presented in Figure 1. The labeling of the atoms is for computational convenience.

2. Vertical Excitations of Reactant. Vertical excitations were calculated for ground-state geometry of reactant 2-methylfuran. They are collected in Table I. The assignments of states is given in the C_{2v} group of furan disregarding the effect of the substituent. In the range up to 6.5 eV, this means about 0.5 eV above the experimental absorption maximum, three singlet states R_1, R_2, and R_3 and four triplet states $^3R_1$, $^3R_2$, $^3R_3$, and $^3R_4$ were found. For all these states, excitations from the HOMO, a π MO of a_2 symmetry, had the largest coefficient in the corresponding CI eigenvector.

The sequence of the five highest occupied MOs is the same as in the unsubstituted system and agrees with experiment[23] and ab initio calculations of von Niessen et al.[24] Lower lying MOs were considered as unimportant for the reaction. The virtual MOs have a different sequence from the unsubstituted furan. The sequence of the unsubstituted furan differs also from the ab initio calculation, where the π MOs $3b_1$ and $2a_2$ lie below the σ MOs $7a_1$ and $5b_2$. With SINDO1 we find as sequence for the virtual MOs of furan $7a_1$, $3b_1$, $5b_2$, and $2a_2$. Bond orders[25] and valence numbers[26] for each state were obtained from the occupied MO's by standard procedures.

(22) Salem, L.; Rowland, C. *Angew. Chem.* **1972**, *3*, 86.

(23) de Alti, G.; Decleva, P. *Chem. Phys. Lett.* **1981**, *77*, 413.

(24) von Niessen, W.; Kraemer, W. P.; Cederbaum, L. S. *J. Electron Spectrosc. Rel. Phenom.* **1976**, *8*, 179.

(25) Jug, K. *J. Am. Chem. Soc.* **1977**, *99*, 7800.

(26) Gopinathan, M. S.; Jug, K. *Theor. Chim. Acta* **1983**, *63*, 497, 511.

$^3I_1$

dihedral angle

3 1 4 2   2.1

3 1 4 5   -8.5
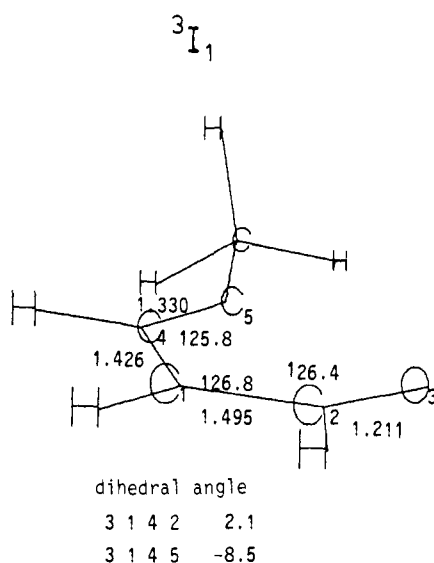
Figure 2. Geometry of diradicaloid $^3I_1$.

Table II. Comparison of Valence Numbers and Net Charges of Reactant R_0 and Diradicaloid $^3I_1$

atom	net charge		valence no.[26]	
	R_0	$^3I_1$	R_0	$^3I_1$
$C_{(1)}$	-0.06	-0.02	3.96	3.42
$C_{(2)}$	+0.19	+0.42	3.90	3.88
$O_{(3)}$	-0.19	-0.27	2.35	1.97
$C_{(4)}$	+0.08	+0.02	3.95	3.75
$C_{(5)}$	+0.20	0.0	3.89	2.62

The state R_1 has A_2 symmetry. It is based on HOMO–LUMO excitation. The LUMO is a σ MO of a_1 symmetry. Since transitions from A_1 to A_2 are dipole forbidden in C_{2v}, the excitation from R_0 to R_1 should show a weak band at best. We obtain R_2 mainly by excitation to the third virtual orbital, a σ MO of b_2 symmetry. The third state R_3 is derived from a $\pi–\pi^*$ excitation into the second virtual MO of b_2 symmetry. In consequence R_3 has B_2 symmetry. Excitation to R_2 is weakly and to R_3 strongly allowed. Below the singlet states we found four triplet states, $^3R_1$, $^3R_2$, $^3R_3$, and $^3R_4$. These belong to the irreducible representations B_2, A_1, A_2, and B_1. Orbital excitations are the same as for the corresponding singlets of the same symmetry. $^3A_1$ is based mainly from HOMO to the fourth virtual MO, a σ MO of a_2 symmetry. Excitations to triplet states should not be observed in the UV absorption spectrum because of change of spin multiplicity.

For the assignment of calculated excitations to the band of the UV spectrum we also used the calculated oscillator strengths. They were in the order of 10^{-3} for R_1 and R_2 and 10^{-1} for R_3. The first two should be weak bands and the third a strong band. The experimental spectrum in methanol[27] shows clearly a weak band at 4.13 eV and a strong band with a maximum at 5.84 eV. The strong band is clearly of B_2 symmetry. The calculated value is 0.48 eV larger than the experimental value in methanol. There is also a gas-phase value of 6.03 eV which is 0.23 eV lower than the calculated value. It is suggestive to assign the weak band at 4.13 eV to R_1 and to compare it with the calculated value of 4.98 eV. We then have to assume that the R_2 value of 5.22 eV corresponds to a weak band which is mostly covered by the slope of the strong band R_3. We tentatively assign a value of 4.90 eV in the experimental spectrum to the R_2 state. The calculated bands are on the average 0.7 eV higher than the experimental ones in solution.

3. Diradicaloid Intermediate. By a linear interpolation between reactant (R_0) and intermediate (I_0) we saw that the lowest triplet approaches the singlet ground state in between these two stationary points. van Tamelen and Whitesides[28] assume that a diradical is generated by the first reaction step, the ring opening. To test this assumption we searched for a diradical. We first found a minimum on the lowest triplet surface (Figure 2). At this point the lowest singlet state is 0.53 eV above the triplet. So a crossing has taken place near by. This situation would refer to a diradical, whereas the minimum $^3I_1$ is just a diradicaloid. van Tamelen and Whitesides have proposed mesomeric structures for the diradical. In this formalism one radical center is atom $C_{(5)}$ and the other is either atom $C_{(1)}$ or O. We have introduced a criterion[29] to

determine radical centers in a molecule. If the valence number of an atom in a molecule is about one unit smaller than the normal valence of this atom, the atom constitutes a radical center. In Table II we compare the valence numbers of reactant R_0 and diradicaloid $^3I_1$. According to the criterion the radical centers are atoms $C_{(1)}$ and $C_{(5)}$. If the valence of an atom is smaller than its normal valence, this means that this atom has free valence. There is a possibility and tendency to form further covalent bonds. Since atoms $C_{(1)}$ and $C_{(5)}$ have free valences, a bond $C_{(1)}–C_{(5)}$ can be formed. In this way the intermediate cyclopropenecarbaldehyde (I_0) can be formed. Here also the valence of oxygen is reduced compared to that of the reactant. If we compare the charge distribution of the diradicaloid ($^3I_1$) with the one of the reactant (R_0), we observe a stronger polarization of the C–O bond in the diradicaloid. The valence numbers,[26] however, are a measure of the covalent bonds formed by the atom. Polarization of the bond reduces covalent bonding, hence the corresponding valence numbers. In this way the reduced valence of oxygen in the diradicaloid can be traced to the polarization of the $C_{(2)}$–O bond.

4. Excited States in the Franck–Condon Zone. In this section we describe the behavior of excited states in the Franck–Condon zone, because the processes in the Franck–Condon zone play an important role in the reaction. A linear interpolation between reactant (R_0) and diradicaloid ($^3I_1$) showed that the reaction cannot take place on the singlet surface R_3 to which excitation takes place, because its energy increases in the direction of the diradicaloid. There must be radiationless transition to another potential surface. The next lower state is R_2. The radiationless transition probability will be increased if surfaces approach each other more closely, i.e., if R_3 descends or R_2 ascends. To test the possibility of lowering R_3 we optimized its geometry, but only a very flat minimum was found. The geometry of this minimum is distinguished from that of the ground state mainly by the tilting of the oxygen atom out of the plane (Table III). The energy of R_2 at the minimum of R_3 is 5.8 eV. It is therefore higher than at the ground-state geometry and the energy difference between R_2 and R_3 is only 0.4 eV. A radiationless transition from a state with B_2 symmetry to a state with B_1 symmetry is allowed by an A_2 vibration during which atoms $C_{(2)}$ and $C_{(5)}$ are moved out of the plane $C_{(1)}C_{(4)}O$ in opposite directions. For nonplanar distortions of the ring there is little energy change for R_3, but a substantial increase for R_2. For a nonplanar distortion with bond lengths, angles, and absolute values of dihedral angles but with atoms $C_{(2)}$ and $C_{(5)}$ tilted out of the plane in opposite directions (Table III), the energy of R_2 is only 0.3 eV below that of R_3. This point B and all others described in this section and therefore the reaction pathway in the Franck–Condon zone are presented in the lower portion of the coordinate diagram (Figure 3). Point A refers to the reactant (R_0), point G to the diradicaloid ($^3I_1$), and point H to the intermediate (I_0). A further distortion in the same direction leads to an avoided crossing $R_{2,3}$ of R_3 and R_2 (Figure 4). Internal conversion takes place so that the system is eventually in the second excited singlet state (point B, Figure 3).

Also the potential energy of R_2 is increasing strongly in the direction of the diradicaloid ($^3I_1$). This means that the reaction cannot take place on this surface. To find the crossing points with
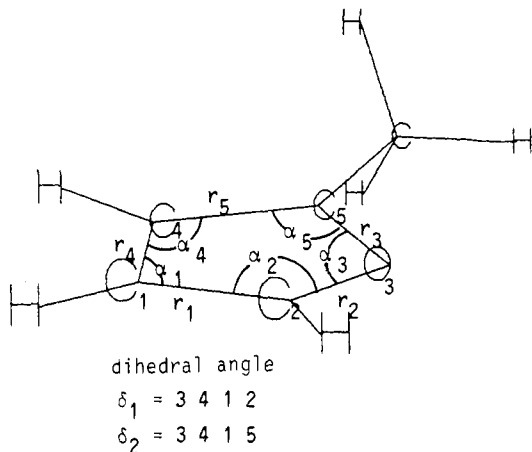
(27) Sadtler UV-Spektren SAD 82 (1962).

(28) van Tamelen, E. E.; Whitesides, T. H. *J. Am. Chem. Soc.* **1971**, *93*, 6129.

(29) Jug, K. *Tetrahedron Lett.* **1985**, *26*, 1437.

(30) Gardner, P. J.; Kasha, M. *J. Chem. Phys.* **1969**, *50*, 1543.

(31) Michl, J. *Excited States in Quantum Chemistry*; Nicolaides, C. A., Beck, D. R., Eds.; Reidel: Dordrecht, 1978; p 417–435.

Table III. Geometries of Minima of Excited States in the Franck–Condon Zone and at Crossing of R_2/R_3 Surfaces

dihedral angle

$\delta_1 = 3\ 4\ 1\ 2$

$\delta_2 = 3\ 4\ 1\ 5$

	r_1	r_2	r_3	r_4	r_5	α_1	α_2	α_3	α_4	α_5	δ_1	δ_2
R_0	1.383	1.390	1.406	1.482	1.401	105.6	111.6	107.3	106.6	109.3	0.0	0.0
R_3	1.442	1.373	1.409	1.424	1.455	102.5	115.6	96.0	103.0	111.9	−7.6	−1.2
$R_{2,3}$	1.442	1.373	1.409	1.424	1.455	102.5	115.6	96.0	103.0	111.9	−8.2	14.7
R_2	1.480	1.356	1.378	1.418	1.446	103.4	112.1	106.3	107.1	110.8	2.9	−0.2
R_1	1.461	1.316	1.432	1.391	1.503	104.7	112.9	108.6	108.3	105.1	2.1	1.5
$^3R_3$	1.476	1.351	1.374	1.414	1.472	103.6	112.5	106.7	106.7	110.1	2.3	0.6
$^3R_2$	1.460	1.314	1.435	1.389	1.503	104.8	113.1	108.3	108.0	105.4	−2.1	−1.9

Figure 4. Location of states during A_2 viration: (- - -) singlet and (- -) triplet.
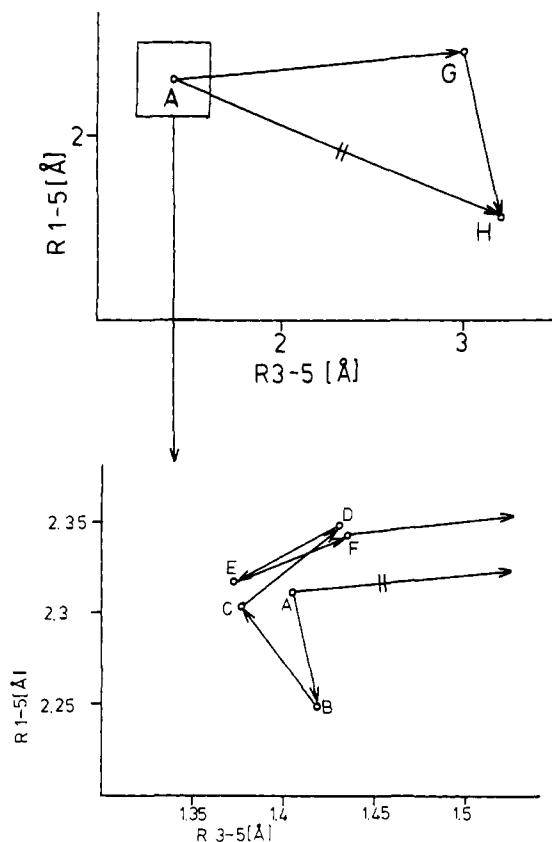
Figure 3. Reaction pathway in the R_{3-5}, R_{1-5} coordinate system; $A = R_0$; $B = R_{2,3}$; $C = R_2$; $D = R_1$; $E = {}^3R_3$; $F = {}^3R_2$; $G = {}^3I_1$; and $H = I_0$.

lower lying surfaces we searched for the minimum of R_2. Such a minimum exists in the Franck–Condon zone (point C, Figure 3). Its geometry is presented in Table III. The energy of this minimum is at 5.08 eV (Figures 5 and 6). The molecule is nearly planar. Compared to the geometry of the ground state, the $C_{(1)}C_{(2)}$ and the $C_{(4)}C_{(5)}$ distances lengthened. For this geometry the energy of the lowest excited singlet R_1 is at 5.00 eV. The energy difference of R_2 and R_1 is only 0.08 eV. A radiationless transition from a B_1 to an A_2 surface can be facilitated by a B_2 vibration. For the geometry of the minimum of the R_2 surface the conse-
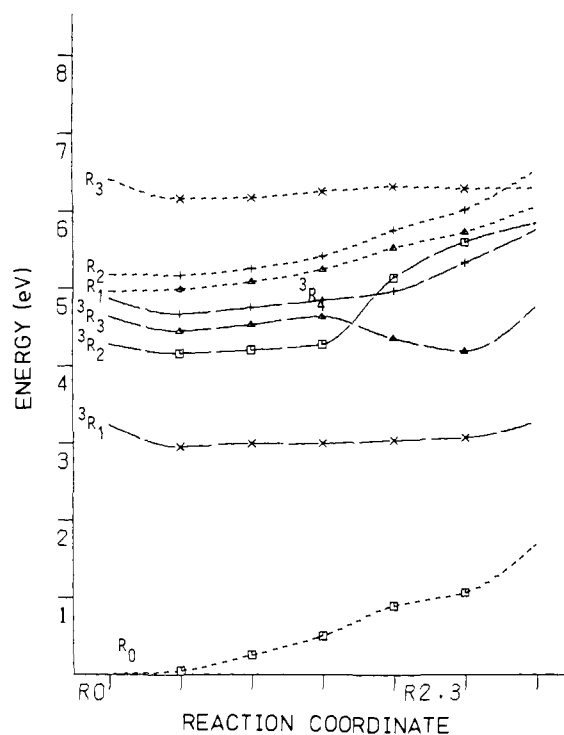
quences of a B_2 vibration on the location of potential energy surfaces were tested. We simulated a B_2 vibration by lengthening the distances $C_{(1)}C_{(2)}$ and $C_{(2)}O$ and shortening the distances $C_{(4)}C_{(5)}$ and $C_{(5)}O$ (point C, Figure 3). For this vibration an avoided crossing takes place which enables internal conversion.

To follow the reaction further, we optimized also state R_1 (point D, Figure 3). The energy decreased to 4.51 eV. At this minimum of R_1 the loss of C_{2v} symmetry is particularly striking. The bonds to the substituted carbon atom $C_{(5)}$ are distinctly longer than those to the opposite unsubstituted carbon atom $C_{(2)}$. The $C_{(5)}O$ bond is 1.432 Å compared to 1.316 Å of the $C_{(2)}O$ bond. It is the weakest bond in the ring with a bond order[25] of 1.25 compared to 1.60 of the $C_{(2)}O$ bond (Table IV). By this distinct difference between the C–O bond lengths in the lowest excited singlet, the
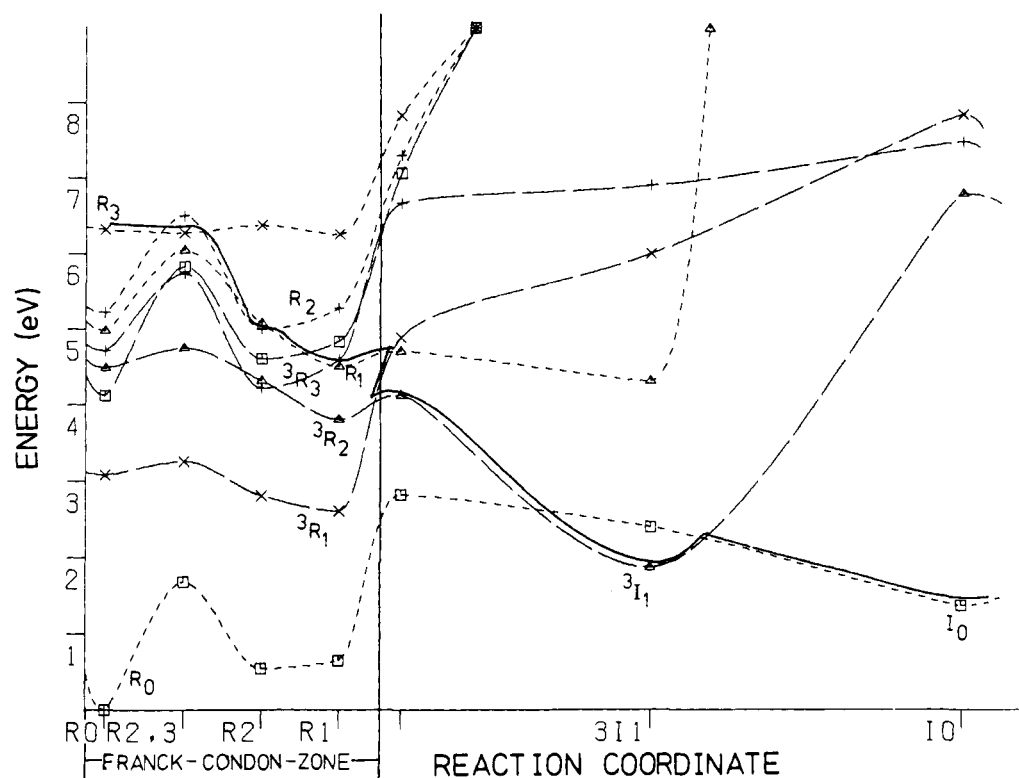
Figure 5. Reaction profile without R_1-$^3R_3$ transition: (---) singlet, (—) triplet, and (—) reaction pathway.
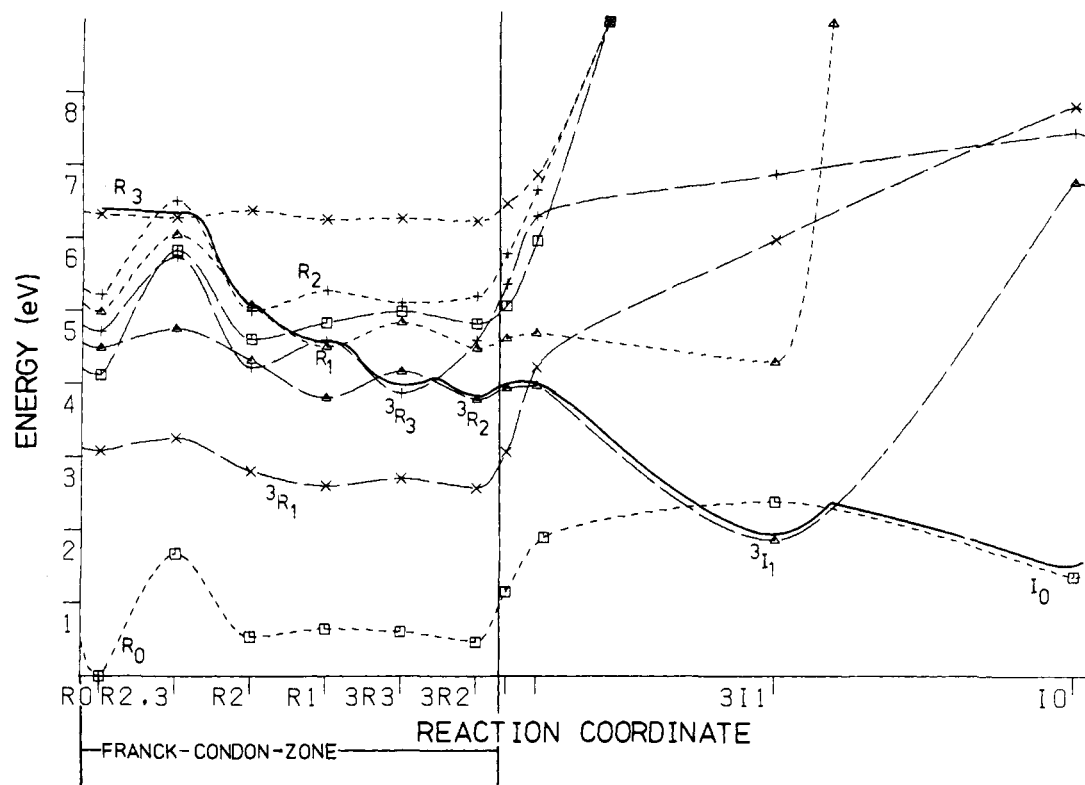

Figure 6. Reaction profile with R_1-$^3R_3$ transition: (---) singlet, (--) triplet, and (—) reaction pathway.

high selectivity of bond breaking as the first step of the reaction can be explained.

We see in the reaction profile (Figures 5 and 6 and Table V) that a triplet state is 0.1 eV above R_1 at the R_1 minimum geometry. So these states are almost degenerate. A transition between states of different spin multiplicity can be achieved by spin–orbit coupling. Spin–orbit coupling can occur between two states if the matrix element
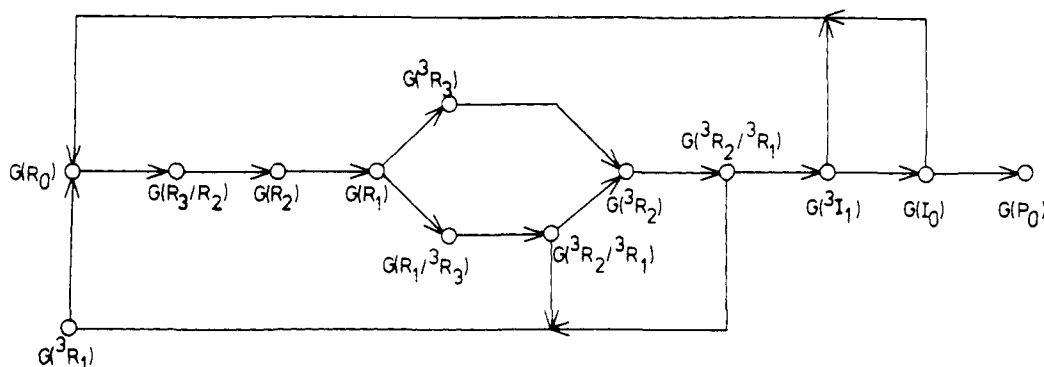
$$\langle \Psi_S | \hat{H}_{SO} | \Psi_T \rangle$$

Table IV. Comparison of Bond Orders of Reactant R_0 and Excited States R_1 and $^3R_2$

	bond order[25]		
bond	R_0	R_1	$^3R_2$
1–2	1.96	1.64	1.62
1–4	1.49	1.80	1.81
2–3	1.43	1.60	1.61
5–3	1.40	1.25	1.24
4–5	1.92	1.39	1.40

Table V. Calculated Energies (eV) of States Participating in the Reaction

state	optimized geometry								
	$G(R_0)$	$G(R_{2,3})$	$G(R_2)$	$G(R_1)$	$G(^3R_3)$	$G(^3R_2)$	$G(^3I_1)$	$G(I_0)$	$G(P_0)$
R_0	0.00					0.47	2.41	1.38	
$^3R_1$	3.08					2.59	1.88	6.83	
$^3R_2$	4.12				4.18	3.80	6.02		
$^3R_3$	4.48			4.60	3.88				
$^3R_4$	4.71			4.84					
R_1	4.98		5.08	4.51					
R_2	5.22	6.51	5.00						
R_3	6.32	6.32							
P_0									0.2

Figure 7. Reaction scheme: G(R) = geometry of minimum of R, and $G(R_a/R_b)$ = geometry of crossings of R_a with R_b.

does not vanish.[32-34] $\hat{H}_{SO}$ is the spin–orbit operator, Ψ_S is the wave function of the singlet state, and Ψ_T is the wave function of the triplet state. The spin–orbit operator has the following form

$$\hat{H}_{SO} = \lambda(r)\hat{L}\cdot\hat{S} = \lambda(r)(\hat{L}_x\hat{S}_x + \hat{L}_y\hat{S}_y + \hat{L}_z\hat{S}_z)$$

$\hat{L}$ refers to the orbital angular momentum and $\hat{S}$ to the spin. Spin–orbit coupling can occur only if one of the direct products of the irreducible representations

$$\Gamma(\Psi_S) \times \Gamma(\hat{L}_i) \times \Gamma(\Psi_T) \quad i = x, y, z$$

contains the totally symmetric representation.[33] In the point group C_{2v}, $\hat{L}_x$ transforms like B_2, $\hat{L}_y$ like B_1, and $\hat{L}_z$ like A_2.[31] R_1 belongs to A_2 and $^3R_3$ to B_1. Since

$$A_2 \times B_2 \times B_1 = A_1$$

intersystem crossing between R_1 and $^3R_3$ is possible.

Now the system is in the triplet state $^3R_3$. This state was also optimized. At its minimum geometry (point E, Figure 3) the formerly second triplet state lies 0.3 eV above the original $^3R_3$. A coupling between the two states with symmetries $^3B_1$ and $^3A_2$ is possible by a B_2 vibration. The pathway from the minimum of R_1 to the minimum of $^3R_3$ corresponds to such a vibration, because the lengths $C_{(1)}C_{(2)}$ and $C_{(2)}O$ become longer and the lengths $C_{(4)}C_{(5)}$ and $C_{(5)}O$ shorter. In this way internal conversion between $^3R_3$ and $^3R_2$ can occur. The system is now in the second excited triplet. This belongs to the same symmetry as R_1, namely A_2. The actual reduction of symmetry observed already for R_1 can be seen at the $^3R_3$ minimum from the bond orders of state $^3R_2$. The bond order of the $C_{(2)}O$ bond is larger than that for the $C_{(5)}O$ bond which is the weakest in the ring.

The $^3R_2$ state was also optimized. The geometry of its minimum (point F, Figure 3) is similar to the one of R_1. Also properties

like bond orders[25] are similar (Table IV). This means that the highly selective bond breaking is indicated in this state. In state R_1 the excitation into the virtual MO $7a_1$ has the largest coefficient in the CI eigenvector. The shape of this MO is responsible for the selective bond breaking.
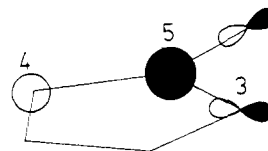
The coefficients of this MO are substantial at atoms $C_{(4)}$, $C_{(5)}$, and $O_{(3)}$ and imply antibonding.

5. Reaction Process. In section III.4 it was shown that a minimum of the first excited singlet state (R_1) is reached in the Franck–Condon zone after vertical excitation of the reactant (R_0) to the third singlet state and subsequent coupling vibrations which enable transitions to lower lying potential surfaces. This reaction pathway in the Franck–Condon zone is represented in the lower portion of the coordinate diagram (Figure 3). The relaxation to the lowest singlet (R_1) reflects the well known fact[31] that after excitation to higher states the first singlet state will be reached in general very quickly, i.e., in picoseconds, by internal conversion. Therefore photochemical reactions occur in general on the first singlet or triplet surfaces.

At the R_1 minimum the reaction pathway branches. This is represented in the reaction scheme in Figure 7. (a) As described in section III.4, one branch leads to the triplet manifold by intersystem crossing and the second triplet state $^3R_2$ is reached. (b) In the second branch, the ring opening starts on the R_1 surface. We tested the behavior of the various potential energy hypersurfaces for this reaction by a linear interpolation between the R_1 minimum and the diradicaloid ($^3I_1$). The energy of the lowest excited singlet (R_1) has barely changed in this direction of the reaction. So the ring opening is possible.

In the course of the ring opening there is a crossing between the first excited singlet state with the second triplet state. During the reaction the ring symmetry is lowered. The point group C_{2v} can no longer be used but must be reduced to C_s. In this group spin–orbit coupling between all singlet and triplet states is allowed. So intersystem crossing is possible at the crossing point. The

(32) McGlynn, S. P.; Vanquickenborne, L. G.; Kinoshita, M.; Carroll, D. G. *Introduction to Applied Quantum Chemistry*; Holt, Rinehart and Winston: New York, 1972.

(33) Hameka, H. F. *Advanced Quantum Chemistry*; Addison-Wesley: Reading, MA, 1965.

(34) Ballhausen, C. J. *Molecular Electronic Structures of Transition Metal Complexes*; McGraw-Hill: New York, 1979.

system is then on the second triplet surface. The minimum of this surface is the Franck–Condon zone. Therefore the pathway from the crossing point of R_1 with $^3R_2$ to the minimum of $^3R_2$ makes a back reaction feasible. On this path there is a crossing with the lowest triplet surface. This belongs to A′ whereas the second triplet belongs to A″. Coupling is possible under an A″ vibration. Such a vibration is a nonplanar distortion. The reaction is connected with such a vibration. Therefore coupling between the surfaces occurs and the system moves to the lower surface.

At the crossing point of $^3R_2$ with $^3R_1$ the system can react in two directions: A minimum of the lowest triplet surface can be reached or the minimum of $^3R_2$. In the second case reaction paths a and b rejoin. In the first case the system can undergo a back reaction to the reactant by phosphorescence. By this possibility the yield is reduced since the reaction is restricted to a photophysical process. It is likely that this branching of the reaction pathway is the reason for the increase of the yield for irradiation in the presence of Hg.[3,5,11,12] In this case the furan molecules are directly excited to a triplet state by collisions with mercury atoms in the triplet state ($^3P_1$). From Figure 7 it is apparent that the first branch of the reaction scheme, which leads back to the reactant, proceeds through a ring opening starting on the lowest singlet surface (R_1). If this singlet state is circumvented by direct excitation to the triplet state, a pathway back to the reactant (R_0) is obstructed. Figure 7 shows that the reaction passes through the minimum of $^3R_2$. To determine the further course of the reaction, a linear interpolation between the $^3R_2$ minimum and the diradicaloid ($^3I_1$) was performed. It showed (Figure 6) that the energy of state $^3R_2$ is lowered in the direction of the diradicaloid. A crossing with the lowest triplet state occurs. As mentioned in the third paragraph of this section, the surfaces couple at this crossing point of $^3R_2$ and $^3R_1$. On the lowest triplet surface the system can proceed to the minimum of the lowest triplet state ($^3R_1$) in the Franck–Condon zone or to the diradicaloid ($^3I_1$).

As can be seen from the reaction profile (Figure 6) the lowest triplet is below the singlet ground state at the geometry of the diradicaloid ($^3I_1$). This means a singlet–triplet crossing has taken place. Since the diradicaloid belongs to point group C_1 without any symmetry, spin–orbit coupling can occur between all singlet and triplet states. So intersystem crossing is possible at singlet–triplet crossing points. On the ground-state surface the system reacts to cyclopropenecarbaldehyde (I_0) or returns to the reactant (R_0). Cyclopropenecarbaldehyde is vibrationally excited. The surface at the minimum is flat. The energy between diradicaloid ($^3I_1$) and intermediate (I_0) is 1.0 eV. Cyclopropenecarbaldehyde can either follow a back reaction to the reactant or react to 3-methylfuran (Figure 7). Since the $C_{(1)}C_{(4)}$ bond in the three-membered ring with a bond order of 1.17 is slight more stable than the $C_{(1)}C_{(5)}$ bond with bond order 1.15, the breaking of the $C_{(1)}C_{(5)}$ bond should be easier than that of the $C_{(1)}C_{(4)}$ bond, so that the back reaction to the reactant should be favored. There are no experimental results about the ratio of these reaction rates. The reaction scheme (Figure 7) shows the various branchings of the reaction pathway. A qualitative estimate on the basis of the many pathways leading back to the reactant results in the con-

clusion that the photochemical isomerization of 2-methylfuran to 3-methylfuran proceeds with low yield. This is in agreement with experiment.

IV. Conclusion

For the photochemical isomerization of 2-methylfuran the vertical excitations of the reactant were calculated first. They were compared with experimental values. With the help of selection rules and oscillator strengths it was established that excitation takes place to the third excited singlet state.

A diradicaloid was found that originates through the ring opening and therefore participates in the reaction.

It was shown that a sequence of radiationless transitions in the Franck–Condon zone initiates the reaction. First there are two internal conversion processes which cause the system to reach the minimum of the lowest excited singlet (R_1). These processes are feasible by vibrations which couple states belonging to different symmetry species. At the R_1 minimum we find the reason for the highly selective bond breaking. The two C–O bonds differ significantly in bond length and bond order. It was shown that there are two reaction pathways at the R_1 minimum which can be followed by intersystem crossing to triplet surfaces. (a) Since the energies of R_1 and the third triplet $^3R_3$ are almost degenerate at the R_1 minimum, intersystem crossing can occur. This is supported by symmetry arguments. By a further internal conversion process the $^3R_2$ minimum is finally reached (upper part, Figure 7). (b) The ring opening can occur on the R_1 surface (lower part, Figure 7), since the energy of the singlet is almost unchanged along this pathway. A crossing of R_1 and $^3R_2$ takes place. It was explained that spin–orbit coupling also makes intersystem crossing feasible in this case. Then an avoided crossing of the second and first triplet surface is reached. The reaction can either lead to the minimum of $^3R_2$ so that pathways a and b are reunited or reach the first triplet state. This alternative leads back to the reactant. Also for the $^3R_2$ minimum the $C_{(5)}O$ bond is considerably weakened compared to the $C_{(2)}O$ bond so that the highly selective bond breaking can take place on this hypersurface.

After the investigation of the process in the Franck–Condon zone the possible reaction pathway to the diradicaloid ($^3I_1$) was shown. The system proceeds on the second triplet surface to the diradicaloid. Internal conversion to the lowest triplet takes place. At the crossing point the system reacts backward or forward to the diradicaloid. Near the diradicaloid, intersystem crossing to the singlet ground state occurs. Again back reaction to the reactant is possible or the intermediate (I_0) cyclopropenecarbaldehyde is reached. On the ground-state surface the intermediate (I_0) can react to form the reactant or the product (P_0).

The small experimental yield is explained by the various branchings of the reaction pathway where in each case one branch leads back to the reactant.